Electron Paramagnetic Resonance and Electron Nuclear Double Resonance Spectroscopies of the Radical Site in Galactose Oxidase and of Thioether-Substituted Phenol Model Compounds

G. T. Babcock,*,† M. K. El-Deeb,†,‡ P. O. Sandusky,†,§ M. M. Whittaker,⊥ and J. W. Whittaker*,⊥

Contribution from the Department of Chemistry, Michigan State University, East Lansing, Michigan 48824, and Department of Chemistry, Carnegie Mellon University, 4400 Fifth Avenue, Pittsburgh, Pennsylvania 15213. *Received September 30, 1991*

Abstract: The organic free radical in galactose oxidase is exchange coupled to the mononuclear copper atom in the active site of the holoenzyme. By removing the copper, the radical can be generated in high concentrations in its electron paramagnetic resonance (EPR)-detectable form. We have carried out a detailed study of the magnetic resonance properties of the radical in the apoenzyme and of a series of phenol model compounds. In the protein, the radical EPR spectrum has partially resolved fine structure with a center crossing at $g = 2.0055$ and an overall peak-to-trough line width of 33 G. The electron nuclear double resonance (ENDOR) spectrum of the radical reveals strong hyperfine couplings to two classes of protons. The first has $A_{iso} = 14.6$ G and tensor components characteristic of a β-proton; the second has $A_{iso} \approx 8$ G and exhibits hyperfine anisotropy typical of an α-proton. Simulation of the radical EPR spectrum with the ENDOR parameters shows that there is only a single proton in each of the two classes of strongly coupled protons. In the weakly coupled region of the ENDOR spectrum, H_2O/D_2O exchange measurements indicate the occurrence of a proton hydrogen-bonded to the phenol oxygen of the radical. In conjunction with earlier data indicating a tyrosine origin for the radical, these observations provide strong experimental support for suggestions that the radical site is the *o*-cysteine-substituted tyrosine residue (Y_{272}) in the immediate coordination sphere of the copper. EPR and ENDOR spectra have been obtained for a series of substituted phenol radicals that support this conclusion. Introduction of a thioether at the ortho position perturbs the **g** tensor and spin density distribution of the phenol moiety only slightly; our ENDOR results indicate, for example, that the spin density at the ring para position is decreased by ~25% upon thioether substitution. The ring thioether substituent is expected to perturb the redox potential of the tyrosine, however, and contribute to the relative ease with which the modified tyrosine in galactose oxidase can be oxidized in comparison with redox-active tyrosines that have been observed in other protein systems.

Introduction

Galactose oxidase is a secreted mononuclear copper enzyme, which has been isolated from the culture media of a number of fungal species.[1] The enzyme from *Dactylium dendroides*, the subject of the work reported here, consists of a single polypeptide of molecular mass 68 000 Da. Even though it contains only a single copper atom, the enzyme catalyzes the two-electron oxidation of the position-6 hydroxyl group of galactose to the corresponding aldehyde, concurrent with the reduction of O_2 to H_2O_2, as follows:

$$RCH_2OH + O_2 \rightarrow RCHO + H_2O_2$$

An unusual property of galactose oxidase, which distinguishes it from simple mononuclear copper enzymes, is that the protein has three well-defined and stable oxidation levels. Of these three, only the intermediate, or one-electron oxidized form, shows a Cu(II) electron paramagnetic resonance (EPR) signal, and this is typical of the type 2 or "normal" class.[2,3] A recent X-ray absorption edge study by Clark et al. has established that the galactose oxidase copper is cupric in the enzyme's highest oxidation level.[4] The fact that this form is EPR-silent indicates that the Cu(II) is antiferromagnetically coupled to a second $S = {}^1/_2$ species. As galactose oxidase contains no other metal besides the redox-active copper, the paramagnetic species to which it is coupled is likely to be an organic radical.

In native galactose oxidase, a minor radical with a distinctive three-line structure is sometimes observed.[3,5] While the amount of this radical in the native enzyme is usually less than 1% of the total enzyme concentration, removal of the copper, followed by treatment with potassium ferricyanide or other oxidants, produces the radical at significantly higher yields, typically between 10% and 40%.[6] Previously, it has been suggested that the galactose oxidase radical is a one-electron oxidized form of pyrroloquinoline quinone (PQQ), a species that has been postulated to exist in a number of redox-active enzymes.[7] Recently, however, Whittaker and Whittaker achieved partial incorporation of methylene-deuterated tyrosine into *D. dendroides* galactose oxidase, and this isotopic enrichment produced a significant perturbation of the apogalactose oxidase radical EPR spectrum.[6] From this result, they concluded that the galactose oxidase radical is not a PQQ species but, rather, that it is metabolically derived from tyrosine, and also that the radical spin is strongly coupled to the proton derived from the tyrosine β-methylene group.

Tyrosines have now been well established as important redox-active cofactors in a number of enzymes.[8] Stable oxidized tyrosine radicals have been identified in the enzymes ribonucleotide reductase (RDPR)[9] and prostaglandin synthase.[10] Two distinct

† Michigan State University.
‡ Present address: Department of Chemistry, University of Alexandria, Alexandria, Egypt.
§ Present address: Department of Biology, The University of Michigan, Ann Arbor, MI 48109.
⊥ Carnegie Mellon University.

(1) (a) Avigad, G.; Amaral, D.; Asensio, C.; Horecker, B. *J. Biol. Chem.* **1962**, *237*, 2736-2743. (b) Aisaka, K.; Terada, O. *Agric. Biol. Chem.* **1982**, *46*, 1191-1197. (c) Koroleva, O. V.; Rabinovich, M. L.; Buglova, T. T.; Yaropolov, A. I. *Prikl. Biokhim. Mikrobiol.* **1983**, *19*, 632-637.
(2) (a) Kosman, D. J. In *Copper Proteins and Copper Enzymes*; Contie, R., Ed.; CRC Press: Boca Raton, FL, 1985; Vol. 2, pp 1-26. (b) Ettinger, M. J.; Kosman, D. J. In *Copper Proteins*; Spiro, T., Ed.; Wiley Interscience: New York, 1982; pp 193-218.
(3) Whittaker, M. M.; Whittaker, J. W. *J. Biol. Chem.* **1988**, *263*, 6074-6080.
(4) Clark, K.; Penner-Hahn, J. E.; Whittaker, M. M.; Whittaker, J. W. *J. Am. Chem. Soc.* **1990**, *112*, 6433-6434.
(5) Winkler, M. E.; Bereman, R. D. *J. Am. Chem. Soc.* **1980**, *102*, 6244-6247.
(6) Whittaker, M. M.; Whittaker, J. W. *J. Biol. Chem.* **1990**, *265*, 9610-9613.
(7) Duine, J. A.; Jongejau, J. A. *Annu. Rev. Biochem.* **1989**, *58*, 403-426.
(8) (a) Prince, R. *Trends Biochem. Sci.* **1988**, *13*, 286-288. (b) Stubbe, J. *Annu. Rev. Biochem.* **1989**, *58*, 257-285.
(9) (a) Reichard, P.; Ehrenberg, A. *Science* **1983**, *221*, 514-519. (b) Sahlin, M.; Petersson, L.; Gräslund, A.; Ehrenberg, A.; Sjöberg, B.-M.; Thelander, L. *Biochemistry* **1987**, *26*, 5541-5548. (c) Bender, C.; Sahlin, M.; Babcock, G. T.; Barry, B. A.; Chandrashekar, T. K.; Salowe, S. P.; Stubbe, J.; Lindström, B.; Petersson, L.; Ehrenberg, A.; Sjöberg, B.-M. *J. Am. Chem. Soc.* **1989**, *111*, 8079-8083.

0002-7863/92/1514-3727$03.00/0

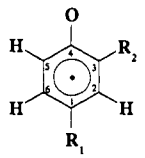

Figure 1. Numbering convention used for tyrosine in this work. R_1 is the $-CH_2CH(NH_2)COOH$ side chain. R_2 is a hydrogen atom in unsubstituted tyrosine, whereas in the galactose oxidase tyrosine 272 radical, R_2 is the $-SCH_2-$ bridge to cysteine 228.

redox-active tyrosines, distinguishable on the basis of their reduction kinetics, occur in the electron transport chains of the photosystem II reaction center complex (PSII), found in all plant and cyanobacterial photosynthetic membranes.[11] Cytochrome *c* peroxidase, under certain conditions, also forms a tyrosine radical, although its catalytic significance is uncertain.[12]

It has been possible to incorporate specifically deuterated tyrosines into *Escherichia coli* RDPR[9] and a cyanobacterial PSII complex.[11] Applying EPR and electron nuclear double resonance (ENDOR) spectroscopies to these isotopically enriched materials has given a detailed understanding of the tyrosine radical spin distributions in these systems. The electronic structures of the PSII and RDPR tyrosine radical species are essentially the same as those of the model tyrosine radicals previously studied by Gordy and co-workers and by Sealy et al.[13] Specifically, the unpaired electron in these radicals resides in an odd-alternant π highest occupied molecular orbital (HOMO), with the major spin concentrations in the p_π orbitals of carbons 1, 3, and 5 (see Figure 1).[14] The EPR spectra of these radicals are thus largely determined by hyperfine coupling to the two ring protons at positions 3 and 5, and to one of the methylene protons that couples to the spin density on carbon 1.[9c,11c] In contrast, there is very little spin density in this orbital at carbons 2 and 6, and the hyperfine couplings from the 2,6 protons are negligible, in terms of their contribution to the line shapes of the EPR spectra. Considering this essential similarity in spin distribution shared by the odd-alternant tyrosine radicals, their EPR spectra show a surprisingly rich variation in width and line shape. This variation in spectral characteristics derives largely from the strong modulation of the hyperfine coupling of the β-methylene proton by the conformation of the methylene group relative to the ring. In essence, the details of the structure of an EPR spectrum from an odd-alternant tyrosine radical are basically defined by the magnitude of the methylene proton coupling.[9,11c]

While it has been established that the galactose oxidase radical shows strong hyperfine structure from a proton metabolically derived from the tyrosine methylene group protons,[6] other properties of the galactose oxidase radical species distinguish it from the odd-alternant tyrosine radicals found in RDPR and PSII. The optical spectrum of the galactose oxidase radical is significantly different from that of the RDPR radical.[6,15] Also, as judged by its reactivity with ferricyanide, the galactose oxidase species appears to have a redox potential of +400 to +500 mV.[6] This is significantly lower than the +930-mV potential of free tyrosine in solution,[16a] or the potentials of the PSII redox-active tyrosines, which are estimated at +760 mV and +1 V.[16b]

Recently, a high-resolution X-ray crystal structure of *D. dendroides* galactose oxidase has appeared that, owing to the crystallization conditions used, probably represents the catalytically inactive form of the enzyme in which the radical site is reduced and diamagnetic.[17] The structure was consistent with the earlier conclusion regarding the absence of PQQ in the enzyme,[6] as no electron density consistent with this cofactor was detected. The ligation sphere of the copper includes two tyrosines, Y_{272} and Y_{495}. Intriguingly, one of these two, Y_{272}, has the ring position-3 proton replaced by the cysteinyl sulfur from C_{228} and thus forms half of a peptide-chain-to-peptide-chain bridge. This tyrosine is further involved in a π stacking interaction with W_{290}. The structural results have led to the suggestions that the galactose oxidase radical either resides on the cysteinyl-substituted Y_{272} or is delocalized over a super π system encompassing Y_{272}, C_{228}, and W_{290}.[17,18]

To extend the earlier spectroscopic work[3,4,6] and to test the above hypotheses for the origin of the galactose oxidase radical, we have carried out a detailed study of the protein-bound free radical and of a series of free radicals derived from substituted phenol model compounds. From our ENDOR spectroscopic results and simulations of EPR line shapes, we conclude that the radical is localized on the ring of Y_{272}. Further, despite the perturbation introduced by the cysteinyl thioether linkage, the substituted tyrosine radical in the apoenzyme has retained an odd-alternant spin distribution, so that the major hyperfine interactions are with one of the methylene protons and the ring position-5 proton.

Materials and Methods

Samples of *D. dendroides* apogalactose oxidase, displaying the radical signal, were prepared as previously described.[6] Total protein concentrations in these samples were 0.8–0.9 mM; the radical concentrations were about 100 μM. Deuterium exchange in these samples was achieved by overnight dialysis (20 h) against 50 mM phosphate buffer, pD 7.0, in D_2O. Phenol, *p*-methylphenol, and *o*-(methylthio)phenol were from Aldrich and were used as supplied. *p*-Methyl-*o*-(methylthio)phenol was synthesized as described,[19] and its structure was confirmed by NMR spectroscopy. Model compound solutions that were used for EPR measurements were prepared by dissolving the respective compound (10 mM) in an aqueous solution of potassium hydroxide (0.1 M). For ENDOR studies, glasses were formed by freezing aqueous solutions of the phenolic compound (10 mM) that contained potassium hydroxide (0.1 M) and lithium chloride (12 M). In all cases, radicals were generated by UV illumination at 77 K,[11c] and the samples were kept in liquid nitrogen until used. Identical EPR spectra were obtained for the phenol models prepared as described above and for samples prepared in benzene, chloroform, or 1 mM aqueous potassium hydroxide. The similarity of these spectra indicates that the various model phenol radicals are not altered by the base concentration present in the aqueous solutions prior to freezing and illumination. The structure of the diamagnetic phenol precursors was also established by NMR spectroscopy on samples prepared in chloroform and in aqueous solutions with different base concentrations. The NMR spectra confirmed that no chemical change was caused by base concentrations in the range used for the EPR and ENDOR samples. Only at high base concentration ($\geq$10 M) did the EPR spectrum of the *p*-methyl-*o*-(methylthio)phenol radical change, and under these conditions it resembled that of the *p*-methylphenol radical.

EPR spectra were taken on a Bruker ER200D spectrometer equipped with a TE_{102} mode cavity. This instrument was also used in conjunction with a Bruker ER250 ENDOR accessory and ER250ENB cavity for ENDOR spectroscopy. Radio-frequency power was provided by an ENI 3100L amplifier driven at frequencies generated by a Wavetek (3000-446) frequency synthesizer.[9c] In-house-built helical ENDOR coils, similar in design to those described in ref 20, were employed. EPR and ENDOR data were acquired by using a Dell 200 AT-compatible microcomputer with an IBM data acquisition board. Precise measurements

(10) (a) Karthein, R.; Dietz, R.; Nastainczyk, W.; Ruf, H. H. *Eur. J. Biochem.* **1988**, *171*, 313–320. (b) Dietz, R.; Nastainczyk, W.; Ruf, H. H. *Eur. J. Biochem.* **1988**, *171*, 321–328. (c) Kulmacz, R. J.; Tsai, A.-L.; Palmer, G. *J. Biol. Chem.* **1987**, *262*, 7719–7724.

(11) (a) Barry, B. A.; Babcock, G. T. *Proc. Natl. Acad. Sci. U.S.A.* **1987**, *84*, 7099–7103. (b) Debus, R. J.; Barry, B. A.; Babcock, G. T.; MacIntosh, L. *Proc. Natl. Acad. Sci. U.S.A.* **1988**, *85*, 427–430. (c) Barry, B.; El-Deeb, M. K.; Sandusky, P. O.; Babcock, G. T. *J. Biol. Chem.* **1990**, *265*, 20139–20143.

(12) Fishel, L. A.; Farnum, M. F.; Mauro, J. M.; Miller, M. A.; Kraut, J.; Liu, Y.; Tan, X.; Scholes, C. P. *Biochemistry* **1991**, *30*, 1986–1996.

(13) (a) Fassanella, E. I.; Gordy, W. *Proc. Natl. Acad. Sci. U.S.A.* **1969**, *62*, 299–304. (b) Sealy, R. C.; Harman, L.; West, P. R.; Mason, R. P. *J. Am. Chem. Soc.* **1985**, *107*, 3401–3406.

(14) (a) Dixon, W. T.; Norman, R. O. C. *J. Chem. Soc.* **1964**, 4857–4860. (b) Carrington, A.; Smith, I. C. P. *Mol. Phys.* **1965**, *9*, 137–147.

(15) Petersson, L.; Gräslund, A.; Ehrenberg, A.; Sjöberg, B.-M.; Reichard, P. *J. Biol. Chem.* **1980**, *255*, 6706–6712.

(16) (a) Harriman, A. *J. Phys. Chem.* **1987**, *91*, 6102–6104. (b) Boussac, A.; Eteinne, A. L. *Biochim. Biophys. Acta* **1984**, *766*, 576–581.

(17) Ito, N.; Phillips, S. E. V.; Stevens, C.; Ogel, Z. B.; McPherson, M. J.; Keen, J. N.; Yadav, K. D. S.; Knowles, A. P. F. *Nature* **1991**, *350*, 87–90.

(18) (a) Thomson, A. J. *Nature* **1991**, *350*, 22–23. (b) McIntire, W. S.; Wemmer, D. E.; Christoserdov, A.; Lindstrom, M. E. *Science* **1991**, *252*, 817–824.

(19) Pilgram, K. H.; Medina, D.; Soloway, S. B.; Gaertner, G. W. U. S. Patent No. 3772391.

(20) Hurt, G.; Kraft, K.; Schultz, R.; Kreilick, R. *J. Magn. Reson.* **1982**, *49*, 159–160.

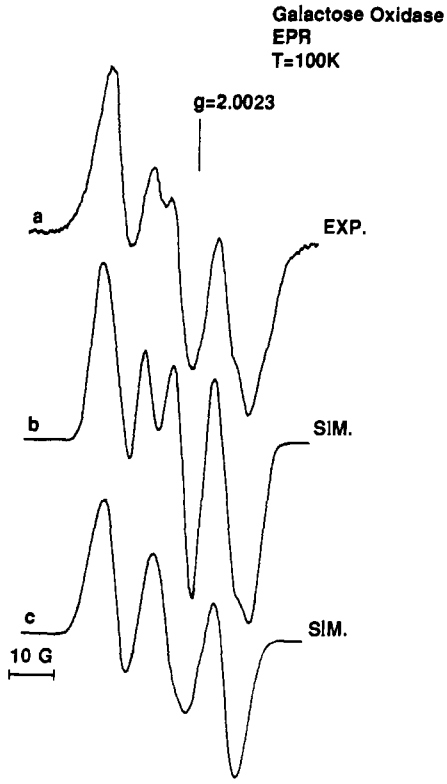

Figure 2. (a) X-band EPR spectrum of ferricyanide-oxidized apogalactose oxidase from *D. dendroides* at 100 K (microwave power 0.65 mW, modulation amplitude 0.5 G). (b) Simulation of the EPR spectrum in (a), with the hyperfine coupling parameters from the ENDOR data for the strongly coupled β-proton (A_{xx} = 15.5 G, $A_{yy} = A_{zz}$ = 14.2 G) and for the ring proton at position 5 (A_{xx} = 11.8 G, A_{yy} = 4.5 G, A_{zz} = 8.5 G) (line width 1.85 G; g_{xx} = 2.0076, g_{yy} = 2.0066, g_{zz} = 2.0023). The **g** tensor was aligned to the molecular axis system such that g_{xx} is along the C–O bond and g_{zz} is perpendicular to the ring plane; the **A** tensor for the β-proton was taken to be coincident with the **g** tensor; the **A** tensor for the ring proton at position 5 was rotated relative to the **g** tensor: A_{xx} and A_{yy} were in the ring plane and perpendicular to and parallel to the C_5–H bond, respectively; A_{zz} was coincident with g_{zz}. (c) Simulation with two nonequivalent isotropically coupled protons, with hyperfine couplings of 14 and 8 G (g_{xx} = 2.0070, g_{yy} = 2.0045, g_{zz} = 2.0023; line width 2.5 G).

of microwave frequencies and magnetic field strengths were made by using a Hewlett-Packard 5255A frequency converter/5245L counter and a Bruker ER-035M gaussmeter, respectively. Sample temperatures were regulated by using a Wilmad N_2 flow system and an Omega 199 temperature readout that was referenced to a copper/constantan thermocouple.

Simulations of powder pattern EPR spectra were performed with a program written by Brok et al.[21] that was modified to be run on either a Digital Equipment Corp. PDP11 minicomputer or a 386-based PC.

Results

1. EPR and ENDOR Spectra of the Apogalactose Oxidase Radical: Strongly Coupled Protons. Figure 2a shows the X-band EPR spectrum of the oxidized apogalactose oxidase free radical at 100 K. Despite the fact that the radical is immobilized and anisotropies in **g** and **A** tensors are expected to broaden the spectrum, relatively good resolution of the hyperfine structure is observed.[6] Three partially resolved lines are apparent, with additional substructure on the two at higher field. The low-field-peak-to-high-field-trough line width is ~33 G, indicating relatively strong coupling to two or more protons in the radical. The g value at the zero crossing of the central line is 2.0055.

ENDOR spectroscopy is well suited to the determination of the molecular origin of the radical, as it is capable of providing the hyperfine tensors for the protons that give rise to the partially

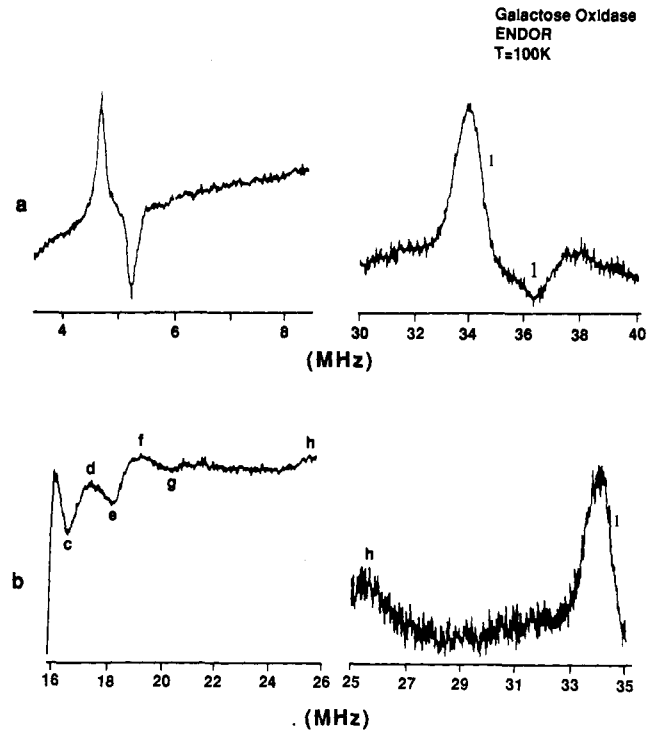

Figure 3. ENDOR spectrum of the apogalactose oxidase radical at 100 K: (a) axial β-proton features; (b) α-proton features. Spectrometer conditions: microwave power, 2.6 mW; rf modulation depth, ±150 kHz; rf power, 100 W at 3 MHz (a, left), 100 W at 30 MHz (a, right), 100 W at 15.8 MHz (b, left), 100 W at 25 MHz (b, right). All spectra are averages of 36 scans each, with the field set at g = 2.0055. Background correction was done by digital subtraction of 36 off-resonance scans with the field set at g = 1.84.

resolved fine structure in the EPR spectrum. The two classes of strongly coupled protons that occur in organic radicals can be distinguished on the basis of these tensors. For α-protons, spin polarization effects dominate the hyperfine interactions, and, as a result, they exhibit large dipolar couplings, with anisotropic hyperfine tensor components comparable to the isotropic coupling. In contrast, hyperconjugation couples β-protons, and they have considerably more isotropic hyperfine tensors.[22] In the RDPR tyrosine radical, for instance, the principal hyperfine tensor components for the 3,5 α-protons are −7.8, −19.7, and −26.9 MHz,[9c] whereas the hyperfine tensor components of the more strongly coupled β-methylene proton are +54.8, +57.8, and +60.0 MHz.[9c] This difference in hyperfine anisotropy is apparent in the ENDOR spectra of radicals immobilized in disordered solids. Moreover, because of their smaller dipolar coupling, β-protons give powder pattern ENDOR features that are narrower, more intense, and, consequently, easier to detect than those of α-protons.

Figure 3 shows the ENDOR spectrum of apogalactose oxidase in several frequency regions. The magnetic field was set at g = 2.0055 in recording the ENDOR spectrum; similar double resonance data were obtained at other field points in the spectrum. Weakly coupled protons occur near the free proton frequency (ν_p = 14.7 MHz) and are discussed in more detail below; resonances from more strongly coupled protons deviate more substantially from ν_p. The ENDOR transitions in this spectrum and in the matrix region in Figure 7, below, are summarized in Table I. In the low- and high-frequency regions of the apogalactose oxidase spectrum (Figure 3a), resonances are observed near 5 and 35 MHz that are characteristic of fairly strong coupling to a proton with an axially symmetric hyperfine tensor in which the anisotropy is

(21) Brok, M.; Babcock, G. T.; DeGroot, A.; Hoff, A. J. *J. Magn. Reson.* **1986**, *70*, 368–378.

(22) (a) Kevan, L.; Kispert, L. *Electron Spin Double Resonance Spectroscopy*; Wiley-Interscience: New York, 1976. (b) Kevan, L.; Narayana, P. A. In *Multiple Electron Resonance Spectroscopy*; Dorio, M.; Freed, J., Eds.; Plenum: New York, 1979; pp 229–259. (c) Kurreck, H.; Kirste, B.; Lubitz, W. *Electron Nuclear Double Resonance Spectroscopy of Radicals in Solution*; VCH Publishers: Berlin, 1988.

Table I. Assignment of the Galactose Oxidase Tyrosine Radical ENDOR Transitions

transition	ν, MHz	proton	tensor component	$\|A\|$, MHz
a',a	13.9, 15.5	H-bonded	$A_\perp$	1.4
b',b	13.5, 15.9	$H_{2,6}$[a]		2.4
c',c	13.2, 16.2	H-bonded	$A_\parallel$	3.1
d	17.1	$H_{2,6}$[a]		4.8
e	18.1	$H_{2,6}$[a]		6.8
f	18.9	H_5	A_y	8.4
g	20.4	$H_{2,6}$[a]		11.4
h	25.5	H_5	A_z	21.6
i	34.6	β-methylene	$A_\perp$	39.8
j	36.4	β-methylene	$A_\parallel$	43.4

[a] The 2,6 proton tensors are unlikely to remain degenerate in the thioether-substituted tyrosine radical (see Table II); assignments of specific resonances to the 2 or 6 protons, however, is not possible at present.[28]

small; the axial line shapes and small hyperfine anisotropy are typical of β-protons. On the basis of this and the magnitude of the hyperfine coupling these lines represent, we conclude that these intense features arise from the tyrosine β-methylene-derived proton, whose coupling to the radical was detected in the earlier EPR study.[6] As there is no intense narrow line near 25 MHz to correspond to the line at 5 MHz, it is clear that this is a case where $A/2 > \nu_p$[23] and that the lines at 5 and 35 MHz represent ENDOR resonances that are centered on $A/2$ and split by $2\nu_p$. From the line shapes, we extract the axial hyperfine tensor components $A_\parallel$ = 43.4 MHz and $A_\perp$ = 39.8 MHz; thus, the isotropic coupling of the tyrosine methylene-derived proton is 41.0 MHz or 14.6 G.

Figure 3b shows the apogalactose oxidase ENDOR spectrum in the 16–35-MHz region. Most of the resonances at frequencies less than 20 MHz arise from weakly coupled protons and are considered below. In the spectrum near 25 MHz, there is a weak derivative-shaped feature (h) that has the line-shape characteristic of the A_z component (in an axis system in which the x- and z-axes are perpendicular to the C–H bond axis and the y-axis is parallel to it) of the hyperfine tensor of a fairly strongly coupled α-proton. For this proton, resonances from the A_y and A_x components are expected near 20 and 30 MHz, respectively.[9c] Resonance f in Figure 3 may represent the lower-frequency feature; we were not successful in unambiguously identifying the higher-frequency component, which may be obscured by the strongly coupled β-proton features above 30 MHz. As noted above, ENDOR lines from α-protons are significantly more difficult to detect in a double-resonance measurement. In the case of the flavin semiquinone bound to riboflavin-binding protein,[24] for example, the α-proton resonances were sufficiently broadened and attenuated by dipolar anisotropies that only features from β-protons and from matrix protons were observed.[22] We were successful in detecting the 3,5 α-proton ENDOR resonances in ribonucleotide reductase, but, here, 1 mM concentrations of the radical were available.[9c] With galactose oxidase, by contrast, the maximal concentration of radical attainable was ~100 μM, which limited our efforts to characterize the α-proton tensor in more detail, even though we varied the measurement temperature from 10 to 100 K and explored a variety of microwave and radio-frequency irradiation conditions.

2. Simulations. ENDOR data provide significant constraints in the simulation of EPR spectra, as they limit the range of values that may be used for the tensor components of strongly coupled nuclei. The double resonance data in Figure 3 demonstrate the occurrence of a β-proton with A_{iso} = 14.6 G in apogalactose oxidase and provide evidence for one or more α-protons with isotropic hyperfine couplings of 7–9 G. These values are typical of tyrosine radicals where the β-proton interaction arises from one of the methylene protons and the α-couplings derive from the 3,5 ring protons. Barry et al., for example, have shown that the neutral tyrosine radical in a rigid aqueous matrix has a methylene proton coupling of 14 G and that A_{iso} for the 3,5 protons is ~7 G.[11c] Nonetheless, the EPR spectral characteristics of the model tyrosine are significantly different from those of the apogalactose oxidase radical: the model shows a single-line, Gaussian-shaped powder EPR signal with a 24-G peak-to-trough line width and partially resolved hyperfine structure;[11c] in contrast, the EPR spectrum in Figure 2a has three resolved lines separated by 11–12 G and a line width of ~33 Gauss. We were unable to simulate the apogalactose oxidase EPR spectrum with any reasonable hyperfine parameter set characteristic of an unperturbed tyrosine radical, i.e., with fairly strong coupling to a β-proton and two α-protons, that was consistent with the ENDOR results. Accordingly, we rule out the possibility that the galactose oxidase radical is localized on tyrosine 495, or any other underivatized tyrosine.

On the basis of the three-line structure of the signal, ^{14}N (I = 1) coupling might be invoked in analyzing the apogalactose oxidase spectrum, were it not for the ENDOR results above and the fact that the three-line structure collapses when methylene-deuterated tyrosine is introduced.[6] Interpretations of the spectrum that involve two equivalent protons can also be ruled out, as such a hyperfine coupling pattern would result in three lines with 1:2:1 relative intensities, while the peak heights of the three lines of the apogalactose oxidase spectrum are approximately equal. A better interpretation, which is suggested by the ENDOR data, involves two nonequivalent proton couplings. In this case, the 14-G methylene proton coupling we observe in the ENDOR spectrum is split by a second proton coupling of 7–9 G. The simulation for this coupling pattern, where both protons are taken as isotropic, is shown in Figure 2c. The two center lines of the four-line hyperfine structure, which arise from transitions that involve the α,β- and β,α-proton spin levels, coalesce into a single line to produce three lines with roughly equal peak heights, split by 11 or 12 G. This simulation reproduces the qualitative features of the protein radical spectrum; however, it does not predict the fine structure on the two higher field lines in the experimental trace. Including the anisotropy expected for the α-proton provides a significant improvement in the simulation. Figure 2b shows that a calculation in which one strongly coupled β-proton and one anisotropically coupled α-proton with hyperfine tensors consistent with the ENDOR results above reproduces the line shape, crossover g value, and hyperfine splittings observed in the apogalactose oxidase spectrum.

The above analysis indicates that the radical observed in oxidized apogalactose oxidase shows strong coupling to two protons, one of which exhibits a hyperfine tensor characteristic of a β-proton, the other of which has a tensor typical of a ring α-proton. Accordingly, and in agreement with the earlier deuteration work,[6] the radical may be assigned to the oxidation product of tyrosine 272, the tyrosine that forms half of the tyrosine–cysteine bridge. The hyperfine couplings that determine the structure of the EPR signal are, thus, the 14.6-G, nearly isotropic coupling from one of the two methylene protons and the anisotropic coupling to the 5-position proton, the position-3 proton having been substituted by cysteinyl sulfur (see Figure 8, below). Our results also indicate that the radical resides mainly on the tyrosine ring and that it retains, to a large degree, the odd-alternant spin density distribution characteristic of an unperturbed tyrosine radical.

3. EPR and ENDOR of Model Phenols. The sulfur substitution at the phenol periphery might be expected to perturb the radical spectrum more substantially than is observed in Figure 2a, particularly as the X-ray structure indicates that partial double-bond character occurs for the ring carbon–sulfur bond in the copper-containing holoenzyme.[17] This bonding arrangement would be expected to locate unpaired electron spin density at the sulfur and perturb the g tensor accordingly. In order to probe the effect that an o-cysteinyl linkage has on the electronic structure and the EPR properties of the tyrosine radical in galactose oxidase, we generated

(23) Proton ENDOR spectra depend on the magnitude of A, the hyperfine coupling constant. If $A/2 < \nu_p$, where ν_p is the proton Larmor frequency, then the ENDOR spectrum shows two lines centered on ν_p, and split by A. For more strongly coupled protons that have $A/2 > \nu_p$, the ENDOR spectrum contains two lines that are centered on $A/2$ and split by $2\nu_p$.[22] Both cases occur in the proton ENDOR spectrum of the apogalactose oxidase radical.

(24) Bretz, N. H.; Heuzel, W.; Kurreck, H.; Muller, F. *Isr. J. Chem.* **1989**, *29*, 49–55.

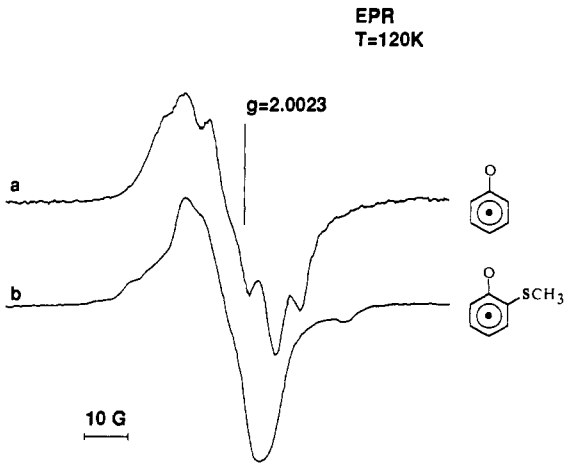

Figure 4. X-band EPR spectra of the frozen radicals of (a) phenol and (b) *o*-(methylthio)phenol (temperature 120 K, microwave power 0.5 mW, modulation amplitude 0.5 G).

Table II. Isotropic *g* Values and Proton Hyperfine Couplings (G) for Substituted Phenoxyl Radicals[a]

compd	g_{iso}	A_m	A_p	A_m'	A_o	ref
phenol	2.0043	1.9	10.2	1.9	6.6	38
o-CH_3	2.0043	1.9	11.5	1.9	6.0	32a, 39, 40
o-F	2.0048	1.4	10.0	2.2	5.8	32b, 41
o-Cl	2.0054	2.0	9.8	1.6	6.0	32a,b
o-OCH_3	2.0043	1.9	8.7	0.0	4.3	42, 43
o-$COCH_3$	2.0045	1.5	10.1	2.2	7.2	32a,b
o-CN		1.4	10.1	2.1	7.1	44
o-CHO		1.7	10.0	2.0	7.1	32a
o-NO_2	2.0050	1.2	10.4	2.2	7.5	32a,b
o-CF_3	2.0047	1.4	10.5	2.2	7.5	32b
o-OH		1.7	8.2	0.2	4.0	43, 45
o-COO^-	2.0048	1.8	10.0	1.8	6.4	38
o-COOH		1.3	10.8	2.2	7.5	41
p-CH_3		1.4	12.3	1.4	6.1	46

[a] For phenol, the ortho positions correspond to positions 3 and 5 in our tyrosine numbering system, the meta positions correspond to positions 2 and 6, and the para positions correspond to position 1 (Figure 1). Values of A_o given in this table are for one ortho proton in all ortho-substituted compounds, and for the two ortho protons in phenol and *p*-methylphenol. For compounds in which an ortho substituent removes the meta proton degeneracy, A_m denotes the coupling to the proton adjacent to the non-proton substituent; A_m' denotes the second meta proton coupling.

a series of phenol radicals in vitro, with and without alkylthio substitution. The alkylthio-substituted compounds are expected to duplicate the planar arrangement of the side chain, with respect to the phenol headgroup[25] that was observed in the crystal structure of the enzyme.[17]

Figures 4 and 5 show the X-band EPR spectra of these radicals in rigid matrices at 120 K. The powder spectrum of phenol radical (Figure 4a) shows a partially resolved five-line structure. This is consistent with the expected unpaired electron spin density distribution for this radical, with large spin density at the para position and smaller spin densities at the ortho positions (Table II). Thus, the features produced by the coupling to the para proton are further split by the two ortho protons, giving rise to the spectrum in Figure 4a. The 10-line spectrum of *p*-methylphenol (Figure 5a) is produced by a large coupling to the methyl protons and a smaller, but appreciable, coupling to the two ortho protons. In solution, these couplings are expected to give rise to a 12-line spectrum; in the powder spectrum in Figure 5a, however, anisotropy in both **g** and **A** tensors produces line broadening and spectral overlap so that only 10 lines are clearly discernible. The coupling to the ring meta protons in small for both phenol radicals,

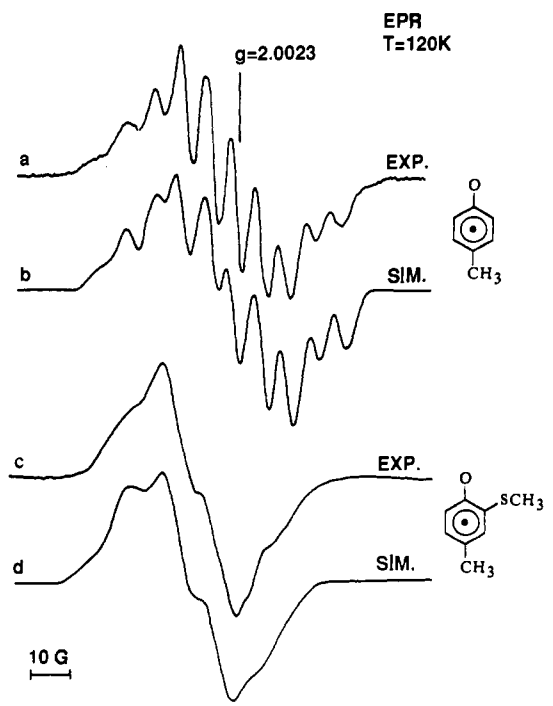

Figure 5. X-band EPR spectra of the frozen radicals of *p*-methylphenol (a) and *p*-methyl-*o*-(methylthio)phenol (c) at 120 K. Traces b and d are computer simulations of the spectra in (a) and (c), respectively. Experimental conditions are the same as in Figure 4. Simulation parameters (b): three equivalent β-protons (A_{xx} = 13.2 G, $A_{yy} = A_{zz}$ = 12.0 G) and two sets of two equivalent α-protons each (A_{xx} = 9.75 G, A_{yy} = 3.25 G, A_{zz} = 6.5 G; A_{xx} = 2.55 G, A_{yy} = 0.8 G, A_{zz} = 1.7 G); line width 1.6 G; g = 2.006, g_{yy} = 2.005, g_{zz} = 2.0023. Simulation parameters (d): three equivalent β-protons (A_{xx} = 9.86 G, $A_{yy} = A_{zz}$ = 9.0 G), two equivalent meta protons (A_{xx} = 2.55 G, A_{yy} = 0.85 G, A_{zz} = 1.7 G), and one ortho proton (A_{xx} = 7.5 G, A_{yy} = 2.5 G, A_{zz} = 5 G); line width 2.5 G; g_{xx} = 2.0095, g_{yy} = 2.0067, g_{zz} = 2.0023.

and these two nuclei contribute only to the line broadening. Substitution of a methylthio group at the ortho position (Figures 4b and 5c) eliminates the moderately strong coupling to the proton in this position, and some of the features resolved in Figures 4a and 5a collapse. Accordingly, the EPR spectral width of the sulfur-substituted compounds is less than that of the corresponding underivatized radical. The *g* values measured at the zero crossing for the spectra shown in Figures 4 and 5 are 2.0054 (Figure 4a), 2.0057 (Figure 4b), 2.0060 (Figure 5a), and 2.0059 (Figure 5c). Qualitatively, the small shift in the *g* value in the methylthio derivatives relative to the unsubstituted compounds indicates that the sulfur substituent does not severely perturb the spin density distribution of the radical.

To test the effect of *o*-cysteinyl substitution on the spin density distribution of phenol- and tyrosine-like radicals quantitatively, we used ENDOR spectroscopy to measure the methyl proton splittings in the *p*-methylphenol and *p*-methyl-*o*-(methylthio)-phenol radicals. The ENDOR data are shown in Figure 6. Both radicals show axial line shapes, typical of the β-proton coupling from a methyl group undergoing free rotation about the carbon–carbon bond.[22a,26] The axial line shape in the spectrum of *p*-methylphenol (Figure 6a) yields transitions at 31.5 MHz ($A_\perp$) and 33.2 MHz ($A_\parallel$) that are assigned to the *p*-methyl group. This is a case where $A/2$ is larger than the proton Larmor frequency (14.7 MHz)[23] and the transitions observed in Figure 6a provide hyperfine coupling values for the methyl protons in *p*-methylphenol as follows: $A_\parallel$ = 37.0 MHz; $A_\perp$ = 33.6 MHz; A_{iso} = 34.7 MHz = 12.4 G. The isotropic hyperfine coupling for the methyl protons determined here by ENDOR for the radical in a frozen matrix is in good agreement with the solution value (Table II), which indicates, as has been observed for several other organic radicals,[22,26] that immobilization does not perturb the spin density

(25) (a) Bernardi, F.; Mangini, A.; Guerra, M.; Pedulli, G. F. *J. Phys. Chem.* **1979**, *83*, 640–643. (b) Ichikawa, T.; Aoki, K.; Iitaka, Y. *Acta Crystallogr.* **1978**, *B34*, 2336–2338.

(26) O'Malley, P. J.; Babcock, G. T. *J. Chem. Phys.* **1984**, *80*, 3912–3913.

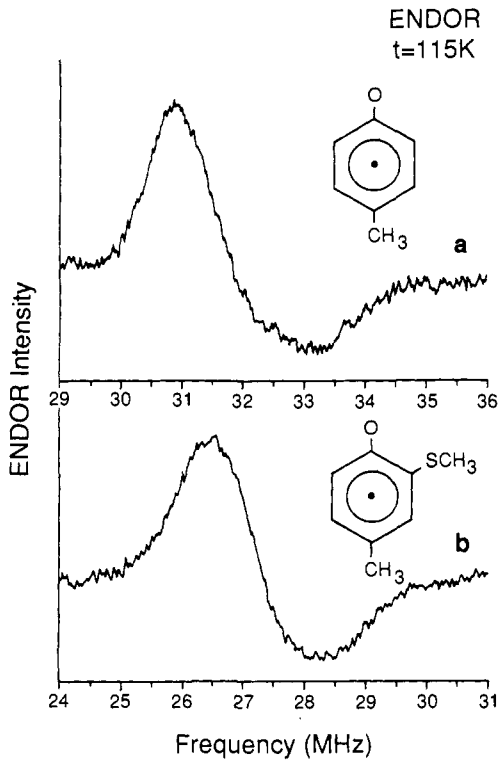

Figure 6. ENDOR spectra of the radicals derived from *p*-methylphenol (a) and *p*-methyl-*o*-(methylthio)phenol (b) at 115 K. Spectrometer conditions: microwave power, 10 mW; rf modulation depth, ±150 kHz; rf power, 40 W at 27 MHz (a) and 40 W at 24 MHz (b). Each spectrum is an average of 64 scans, with the field set at the zero crossing of the EPR spectrum. Background correction was done as in Figure 3.

distribution and hyperfine coupling significantly. For *p*-methyl-*o*-(methylthio)phenol (Figure 6b), an axial proton ENDOR line shape is observed with transitions corresponding to $A_\perp$ and $A_\parallel$ at 27.1 and 28.3 MHz, respectively. From these values we obtain $A_\perp$ = 25.2 MHz, $A_\parallel$ = 27.6 MHz, and A_{iso} = 26.0 MHz = 9.3 G. For neither sulfur-substituted model were we able to detect the coupling to the ortho position α-proton by ENDOR, despite the fact that the spectral simulations below indicate a substantial coupling to this proton.

The data in Figure 6 show that the methyl proton coupling at the para position decreases by ~25% when one of the protons ortho to the hydroxyl group is substituted by a thioether linkage. Assuming that sulfur substitution induces no drastic change in the McConnell Q value, we interpret this result to indicate a corresponding reduction in spin density at the para position. Using the ENDOR data for the methyl protons and hyperfine tensor components for the ortho protons consistent with their α-proton character and with their isotropic coupling constants (Table II), good simulations of the spectra of *p*-methylphenol and its thioether derivative are obtained (Figure 5b,d).

4. ENDOR Spectrum of the Apogalactose Oxidase Radical: Weakly Coupled Features and Evidence for a Hydrogen-Bonded Proton. In the few cases where hydrogen-bonded proton hyperfine interactions have been studied by ENDOR,[27] it has been found that the hyperfine tensors from hydrogen-bonded protons are, as a class, axial and purely dipolar. The case of *p*-benzoquinone radical anion is typical. The radical is hydrogen bonded at the oxygens, and ENDOR spectroscopy of powder samples resolves the principal hyperfine components of the hydrogen-bonded protons as A_z = +5.9 MHz and $A_x = A_y$ = −2.8 MHz.[27a] The principal tensor components sum close to zero, which is characteristic of purely dipolar coupled protons, and should be a property common to protons hydrogen bonded to a radical in a similar manner.

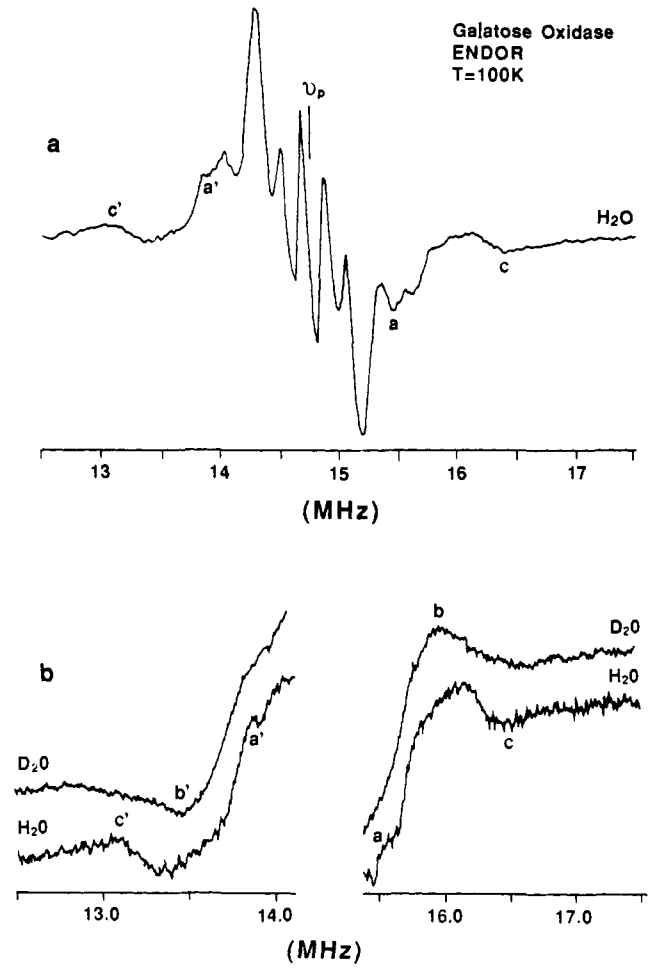

Figure 7. ENDOR spectrum of the apogalactose oxidase radical, showing the weakly coupled proton features: (a) spectrum of the enzyme isolated in H_2O buffer; (b) expansion of the spectrum of the enzyme in H_2O buffer (lower trace) and the corresponding spectrum of the D_2O-dialyzed enzyme (upper trace) (temperature 100 K, microwave power 2.6 mW, rf modulation depth ±37.5 kHz, rf power 100 W at 12.5 MHz). Each spectrum is an average of 36 scans. Background correction was done as in Figure 3.

Figure 7a presents the weakly coupled proton ENDOR spectrum. The features at 13.2 and 16.2 MHz, in the expanded spectrum in Figure 7b, are of particular interest. In the enzyme in H_2O buffer, these features appear to be derivative in shape. Dialyzing the enzyme against D_2O phosphate buffer (pD 7) overnight, however, produces a significant change in their appearance. The derivative-shaped line at 13.2 MHz loses its positive excursion and becomes a negative feature that peaks at 13.5 MHz (b′) following exchange, while the derivative-shaped line at 16.2 MHz loses its negative excursion and becomes a positive feature peaking at 15.9 MHz (b). Thus, the derivative line shape arises from superimposed features from two different classes of protons, only one of which is exchangeable with solvent protons. The dialysis against D_2O also produces significant changes at 13.9 and 15.5 MHz (a′ and a). The D_2O-induced change in the spectrum at these points is consistent with the disappearance of derivative-shaped features superimposed on other unresolved resonances. Thus, there are two sets of D_2O suppressible ENDOR features, and we conclude that the axial features at 13.2 and 16.2 MHz and the derivative-shaped features at 13.9 and 15.5 MHz derive from coupling to one weakly bonded, dipolar-coupled proton, with principal hyperfine tensor components of A_z = +3.1 MHz and $A_x = A_y$ = −1.4 MHz. As Y_{272} ligates the galactose oxidase copper atom in the holoenzyme,[17] it is likely that the hydrogen-bonded proton, detected by ENDOR in the apoenzyme, occupies a position

(27) (a) O'Malley, P. J.; Babcock, G. T. *J. Am. Chem. Soc.* **1986**, *108*, 3995–4001. (b) Muto, H.; Iwasaki, M. *J. Chem. Phys.* **1973**, *59*, 4821–4829. (c) Reddy, M. V. V. S.; Lingam, K. V.; Gundu Rao, T. K. *J. Chem. Phys.* **1982**, *76*, 4398–4405. (d) Fan, C.; Teixeira, M.; Moura, J.; Moura, I.; Huynh, B.-H.; LeGall, J.; Peck, H. D., Jr.; Hoffman, B. M. *J. Am. Chem. Soc.* **1991**, *113*, 20–24.

on the tyrosine oxygen vacated by the holoenzyme copper. If we assume a spin density on the phenol oxygen similar to that obtained earlier for the tyrosine phenol oxygen in RDPR ($\rho_O = 0.16$)[9c], then a dipole–dipole calculation provides a hydrogen bond distance of 2.0 Å, which is typical of biological hydrogen bonds.

In addition to the strongly coupled α- and β-proton features and the resonances from the hydrogen-bonded protons, a number of weakly coupled, low-intensity, α-proton lines are observed in the apogalactose oxidase ENDOR spectrum at frequencies less than 20 MHz (Figure 3b). If the transitons that arise from the hydrogen-bonded proton are corrected for, these weakly coupled features correspond to couplings of 2.4 (b), 4.8 (d), 6.8 (e), 8.4 (f), and 11.4 MHz (g). Resonance f is likely to arise from the A_y tensor component of the ortho proton, as discussed above. On the basis of the magnitudes of the ring proton couplings observed in RDPR,[9c] we assign the other four resonances to the 2,6-position protons. More specific assignment of these features is difficult, in large part because it is unlikely that the 2- and 6-position couplings remain degenerate in the presence of the position-3 cysteinyl substitution (see Table II) and because attempts at specific deuteration at these positions have been unsuccessful.[28]

Discussion

The data presented here show that the apogalactose oxidase free radical has only two moderately strongly coupled protons—one an α-proton, the other a β-proton. The hyperfine coupling constants for these nuclei and the hydrogen-bonding properties of the radical are those expected from an odd-alternant tyrosine radical in which one of the ortho protons has been replaced by a substituent that only weakly couples to the unpaired electron. These results, combined with the deuterium labeling work[6] and the recent X-ray structure,[17] lead to the conclusion that the apogalactose oxidase radical is the thioether-modified tyrosine, Y_{272}, that occurs in the immediate coordination sphere of the mononuclear copper center in the holoenzyme. Two additional lines of evidence place the position of the radical species within the ligand sphere of the holoenzyme copper. First, in the highest oxidation level of the enzyme, the radical antiferromagnetically couples with the Cu(II) $S = {}^1/_2$ to produce an $S = 0$ EPR silent ground state.[3,5] Second, this oxidation level of the enzyme has optical absorption bands that have characteristics suggestive of contributions from tyrosine-to-Cu(II) charge-transfer transitions.[29] However, the Raman spectra associated with these transitions show a systematic shift of the vibrational bands to lower frequencies relative to what is observed in typical copper(II) tyrosinate model spectra, consistent with a heavy atom substituted ring system or a decrease in the tyrosine ring bond order in the galactose oxidase chromophore species, as would be expected for the oxidized form of the tyrosine-derived species.

The analysis of the apogalactose oxidase EPR spectrum indicates that the *o*-cysteinyl substitution has not dramatically disrupted the usual HOMO symmetry observed in tyrosine radicals. This conclusion is consistent with the fairly subtle effects such substitutions usually have on the spin distributions in odd-alternant radical species. Table II includes *g* value and hyperfine coupling data for ortho-substituted neutral phenoxyl radicals. Often, the presence of heavy elements, such as chlorine, bromine, or sulfur, in organic radicals will induce a significant distortion in the **g** tensor components away from the free electron *g* value (2.0023). The cysteine radical, for instance, has principal **g** tensor components of 2.003, 2.029, and 2.052, and $g_{iso} = 2.028$.[30] Heavy element substituents on odd-alternant radicals, however, generally induce **g** tensor distortions of a much smaller magnitude. The g_{iso} values for the *o*-chlorophenoxyl and *p*-(methylthio)benzyl radicals, for instance, are 2.0054 and 2.0049, respectively.[31,32] Thus, the crossover *g* value of the galactose oxidase *o*-cysteinyltyrosine 272 radical, 2.0055, is typical for this class of radicals. Conversely, this *g* value is low, relative to the cysteine radical g_{iso} value, so that it can be argued that the radical is localized mainly on the tyrosine ring, with only slight delocalization of the unpaired electron spin density to the cysteine sulfur.

The geometry of the thioether substituent relative to the phenol ring plane may be expected to influence the extent to which unpaired electron spin density is delocalized to the side chain. In general, conjugative overlap is favored when the –SR group is coplanar with the ring and planar [ring–thioalkyl] structures are observed in the crystal structures of this class of compounds.[25b] The conjugative interaction is considered to be responsible for the planarity of thiophenol; this structure is likely to persist in the neutral radical forms of thioether-substituted phenols.[25a] Thus, the planar [phenol–SCH_2–] structure that Ito et al. found for Y_{272} in the crystal structure of the galactose oxidase holoenzyme[17] most likely represents a low-energy configuration and should be reasonably well reproduced by the model compounds we have studied. Despite the planar structure, however, the EPR spectra of the methylthio-substituted model compounds, Figures 4 and 5, indicate that the thioether substituent introduces only slight perturbations to the **g** tensor of the unsubstituted phenol radical, consistent with the absence of extensive spin delocalization to the side chain. Prince et al. have provided a very useful discussion of the analogous situation for the geometries that occur in methoxy-substituted quinone systems.[33]

The data in Table II show that the model radicals retain the odd-alternant spin distribution, with strong couplings at the ortho and para positions and weak couplings at the meta positions, even when strong electron-donating substituents, such as $-OCH_3$, are present. Likewise, hyperfine data for substituted benzyl radicals indicate that thioether substituents do not strongly perturb spin distributions in odd-alternant species. Benzyl radical and *p*-(methylthio)benzyl radical, for instance, have essentially the same hyperfine couplings at the ortho (5.1 G) and meta (1.7 G) positions.[31] Our EPR and ENDOR data on the model compounds show that the introduction of an *o*-methylthio substituent to the phenol ring in *p*-methylphenol decreases the spin density at the para position by approximately 25%. In galactose oxidase, the extension of the methylthio side chain to include the rest of the cysteine molecule is not expected to change this effect; i.e., we expect the spin density at C1 in the galactose oxidase radical to be ~25% smaller than that in an unsubstituted tyrosine radical. A spin density of 0.49 occurs at C1 of the RDPR tyrosine radical,[9] which is typical of the spin density at this position in phenol radicals. Accordingly, we predict that the spin density at C1 of the galactose oxidase radical will be ~0.37.

In the RDPR case, Bender et al.[9c] were able to carry out a self-consistent determination of the C1 spin density by assessing the contribution of unpaired spin at this position to the observed hyperfine anisotropy of the ortho and meta protons. They then used the C1 spin density and the methylene proton coupling they

(28) In previous EPR/ENDOR studies, incorporation of specifically deuterated tyrosine into *E. coli* and the cyanobacterium *Synechocystis* facilitated the detailed analysis of the proton hyperfine structure in the RDPR and PSII tyrosine radicals.[9c,11c] Attempts to extend this strategy to *D. dendroides* galactose oxidase have met with mixed success. The inhibitor glyphosate can be used to suppress the normal fungal aromatic amino acid metabolism (see Kishore, G. M.; Shah, D. M. *Annu. Rev. Biochem.* **1988**, *57*, 627–663). Inclusion in the culture medium of methylene-deuterated tyrosine, along with undeuterated phenylalanine and tryptophan, then results in a partial isotopic labeling of the fungal tyrosine population and a significant perturbation of the apogalactose oxidase EPR spectrum.[6] Our attempt to extend this result, by using ring-deuterated tyrosine, failed to produce any major modifications to the apogalactose oxidase EPR spectrum. In experiments in which radioactively labeled tyrosine was used, however, we consistently find ~70% incorporation of label. Thus, the absence of detectable perturbation in radical-containing galactose oxidase prepared from ring-deuterated tyrosine may reflect a labilization of ring protons in the biosynthesis of the active site.

(29) Whittaker, M. M.; DeVito, L. V.; Asher, S. A.; Whittaker, J. W. *J. Biol. Chem.* **1989**, *264*, 7104–7106.

(30) (a) Kurita, Y.; Gordy, W. *J. Chem. Phys.* **1961**, *34*, 282–288. (b) Box, H. C.; Freund, H. G.; Budzinski, E. E. *J. Chem. Phys.* **1966**, *45*, 809–811.

(31) Wayner, D. D. M.; Arnold, D. R. *Can. J. Chem.* **1984**, *62*, 1164–1168.

(32) (a) Dixon, W. T.; Moghimi, M.; Murphy, D. *J. Chem. Soc., Faraday Trans. 2* **1974**, 1713–1720. (b) Holton, D. M.; Murphy, D. *J. Chem. Soc., Faraday Trans. 2* **1979**, 1637–1642.

(33) Prince, R. C.; Halbert, T. R.; Upton, T. H. In *Advances in Membrane Biochemistry and Bioenergetics*; Kim, C. H., et al., Eds.; Plenum Press: New York, 1988; pp 469–477.

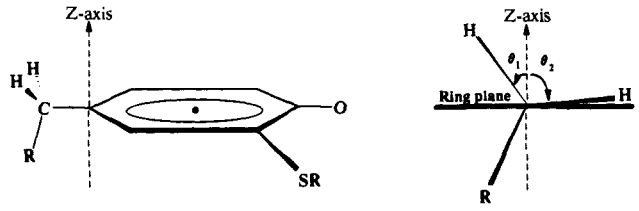

Figure 8. A model for the *o*-cyteinyl-substituted tyrosine radical in apogalactose oxidase: (a) side view; (b) end view, looking along the C_β–C_1 band. The dihedral angle for the more strongly coupled proton, θ_1, is 34°.

measured by ENDOR in an angle-dependent McConnell-type relationship

$$A^{C-H} = \rho_{C1} B \cos^2 \theta$$

to determine the geometry of the β-CH_2 group relative to the tyrosine ring. In the above equation, A^{C-H} is the hyperfine coupling to the β-methylene proton, ρ_{C1} is the spin density at the C1 position, B is a constant equal to 162 MHz, and θ is the dihedral angle between the ring carbon p_z orbital and the C_1–C_β–H plane. The dihedral angle determined from the ENDOR data was subsequently confirmed in the crystal structure of RDPR.[34] For apogalactose oxidase, we used the scaled C1 spin density and the measured β-H hyperfine coupling in the McConnell relationship above to calculate that $\theta = 34°$. This calculation, although crude, suggests that rearrangement of the tyrosine phenol headgroup occurs upon removal of the copper, as the dihedral angle reported by Ito et al.[17] from the crystal structure of the metal-containing protein is 16°. Moreover, from the absence of evidence for strong coupling to the second β-proton in the radical in the apoenzyme, we conclude that the dihedral angle for this proton is close to 90°, from which we deduce the headgroup geometry shown in Figure 8. Comparison with the crystal structure of the holoenzyme suggests, then, that a rotation of ~50° occurs about the C_β–C_1 bond upon removal of the copper ion.

While the magnetic resonance parameters of the odd-alternant tyrosine radical are not strongly perturbed by an *o*-thioether substituent, the chemistry of the tyrosine might be more dramatically affected. The methylthio substituent significantly enhances electrophilic aromatic substitution and hydrogen/deuterium exchange on benzene rings.[35] Although in benzene the methylthio substituent directs electrophilic substitution ortho and para, when other ring substituents are present, substitution can occur meta to the methylthio group. Reactivity effects of this kind could, thus, account for our observation that growth of the *D. dendroides* cultures in the presence of glyphosate and ring-deuterated tyrosine has no effect on the structure of the apogalactose oxidase EPR signal.[28]

The redox potential of apogalactose oxidase tyrosine 272 is approximately +450 mV.[6] This is 250–500 mV lower than the potentials of the redox-active tyrosines in the photosynthetic water-oxidizing complex.[16b] This low potential is understandable, at least in part, as a consequence of the *o*-thioether substitution. Meta- and para-substituted toluenes, which also form odd-alternant radicals, are observed to obey linear Hammett-type relationships, with respect to their redox potentials.[36] In this context, thioether substituents are electron donating and, thus, are expected to lower the redox potential of tyrosine.[31,35] Qualitatively, the same trend is observed in the case of ortho-, meta-, and para-substituted phenols, where electron-donating substituents lower the redox potentials by as much as several hundred millivolts.[37] In this case, however, the ortho-substituted compounds did not follow a simple linear Hammett relationship, and no thioether-substituted compounds were studied. In the light of these studies, we conclude that the *o*-cysteinyl thioether linkage acts as an electron-donating substituent that serves to lower the Y_{272} redox potential. The situation is probably more complex than this, however. It has been suggested, for instance, that a π–π interaction between tryptophan 290 and the tyrosine–cysteine bridge acts to stabilize the radical.[17] It is also likely that the conformations of the $-SCH_2$ and β-CH_2 groups are important in determining the Y_{272} redox potential. This is the case in quinones, where the $-OCH_3$ group conformations strongly modulate the redox potential.[33] Interestingly, the planar geometry that Knowles and co-workers observed for the thioether substituent in the holoenzyme[17] is expected to optimize the influence of this group in stabilizing the radical and lowering its redox potential. However, we note that, in the case of PSII, the two redox-active tyrosines differ in redox potentials by 250 mV, even though their EPR spectra and, therefore, their phenol headgroup β-methylene conformations are identical. Clearly, the interplay of the factors that determine the reduction potentials of the redox-active tyrosine species can be subtle and are not yet well understood. In the case of galactose oxidase, it seems unlikely that the Y_{272} redox potential observed in the apoenzyme is retained in the holoenzyme, as the ligation of Cu(II) no doubt constitutes a significant perturbation.

On the basis of the retention of an odd-alternant spin distribution, we consider galactose oxidase Y_{272} as a redox-active tyrosine similar to those found in PSII, RDPR, and prostoglandin synthase. The galactose oxidase species is the first of these identified in fungal material, so that it now has been established that redox-active tyrosines occur as enzyme cofactors in all five taxonomic kingdoms.

Acknowledgment. This work was supported by grants from NIH (GM37300 to G.T.B.) and NSF (DMB-87/7058 to J. W.W.). We thank Dr. Peter Knowles for a discussion of dihedral angles in the crystal structure of galactose oxidase and Dr. Roger Prince for discussions on the effects of substituent conformations on redox potentials in conjugated ring systems.

(34) Norlund, P.; Sjöberg, B.-M.; Eklund, H. *Nature* **1990**, *345*, 593–598.
(35) Tagaki, W. In *Organic Chemistry of Sulfur*; Oae, S., Ed.; Plenum Press: New York, 1977; pp 231–295.
(36) (a) Russell, G. A.; Williamson, R. C. *J. Am. Chem. Soc.* **1964**, *86*, 2357. (b) Walling, C.; Miller, B. *J. Am. Chem. Soc.* **1957**, *79*, 4181. (c) Pearson, R. E.; Martin, J. C. *J. Am. Chem. Soc.* **1963**, *85*, 3142–3146. (d) Pryor, W. A. *Free Radicals*; McGraw-Hill: New York, 1966.
(37) Bordwell, F. G.; Cheng, J.-P. *J. Am. Chem. Soc.* **1991**, *113*, 1736–1743.
(38) Neta, P.; Fessenden, R. W. *J. Phys. Chem.* **1974**, *78*, 523–529.
(39) Stone, T. J.; Waters, W. A. *Proc. Chem. Soc., London* **1962**, 253–254.
(40) Dixon, W. T.; Murphy, D. *J. Chem. Soc., Faraday Trans. 2* **1976**, 1221–1230.
(41) Stone, T. J.; Waters, W. A. *J. Chem. Soc.* **1964**, 213–218.
(42) Smith, I. C. P.; Carrington, A. *Mol. Phys.* **1967**, *12*, 439–448.
(43) Stone, E. W.; Maki, A. H. *J. Am. Chem. Soc.* **1964**, *87*, 454–458.
(44) Dixon, W. T.; Moghimi, M.; Murphy, D. *J. Chem. Soc., Perkin Trans. 2* **1975**, 1189–1191.
(45) Loth, K.; Graf, F.; Günthard, H. H. *Chem. Phys.* **1976**, *13*, 95–113.
(46) Dixon, W. T.; Norman, R. O. C. *J. Chem. Soc.* **1964**, 4857–4860.